Aalto University
School of Science
Degree Programme in Engineering Physics and Mathematics

Janne Mäntylä

Feasibility of Continuous Respiratory Volume Monitoring with Indirect Measurements

Master's thesis
Espoo, October 10, 2016

Supervisor: Prof. Lauri Parkkonen
Instructor: D.Sc. (Tech.) Kimmo Uutela

Aalto University
School of Science
Degree Programme in Engineering Physics and Mathematics

ABSTRACT OF MASTER'S THESIS

Author:	Janne Mäntylä		
Title:	Feasibility of Continuous Respiratory Volume Monitoring with Indirect Measurements		
Date:	October 10, 2016	**Pages:**	v + 37
Major:	Biomedical Engineering	**Code:**	Tfy-99
Supervisor:	Prof. Lauri Parkkonen		
Instructor:	D.Sc. (Tech.) Kimmo Uutela		

Respiratory rate is a routinely monitored vital parameter in hospitals. Despite the change in respiratory rate often being the first sign of patient deterioration, it is not always a sufficient indicator of patient's ventilatory status. A number of adverse events could be reacted to earlier if also the respiratory volume was monitored.

In this work, feasibility of indirect respiratory volume measurements was assessed. Impedance pneumography (IP) and respiratory inductance plethysmography (RIP) measurement data from 15 measurement sessions with voluntary test subjects were analyzed. Signal amplitude was used to track relative minute-volume values. Furthermore, a signal quality indicator was developed to detect sections of signal where the relative volume estimate was unreliable.

The average coefficient of determination, R^2, for the best RIP signal evaluation method was 0.71 while it was 0.53 for IP. RIP is more accurate than IP, but requires an extra sensor whereas IP can be measured simultaneously with ECG using the same electrodes. The developed signal quality index method improved coefficient of determination between the reference method and IP measurement to $R^2 = 0.66$. The relative volume information is lost with patient posture change, but this change could be detected using other methods. These results show that IP and RIP can detect trends in respiratory volume.

Keywords:	Monitoring, Respiration volume
Language:	English

Aalto-yliopisto
Perustieteiden korkeakoulu
Teknillisen fysiikan ja matematiikan koulutusohjelma

DIPLOMITYÖN TIIVISTELMÄ

Tekijä:	Janne Mäntylä		
Työn nimi:	Hengitystilavuuden jatkuvan seurannan toteutettavuus epäsuorin mittausmenetelmin		
Päiväys:	10. lokakuuta 2016	**Sivumäärä:**	v + 37
Pääaine:	Lääketieteellinen tekniikka	**Koodi:**	Tfy-99
Valvoja:	Prof. Lauri Parkkonen		
Ohjaaja:	TkT Kimmo Uutela		

Hengitystiheyttä seurataan sairaaloissa rutiininomaisesti. Vaikka muutos hengitystiheydessä usein kertoo potilaan tilan heikentymisestä, se ei yksin riitä kuvaamaan potilaan hengityksen tilaa. Useisiin haitallisiin tilanteisiin voitaisiin reagoida aiemmin jos seurattaisiin myös hengitystilavuutta.

Tässä työssä tutkittiin hengitystilavuuden seurannan toteutettavuutta epäsuorin mittausmenetelmin. Impedanssipneumografia- (IP) ja induktanssipletysmografiasignaalit (RIP) mitattiin ja analysoitiin 15 mittauksesta vapaaehtoisilta koehenkilöiltä. Signaalin amplitudin perusteella laskettiin suhteellisia minuuttivolyymiarvoja. Myös signaalin laadun mittari kehitettiin havaitsemaan signaalin sellaiset osiot, joissa arvioitu suhteellinen minuuttitilavuus oli epäluotettava.

Selitysasteen, R^2, keskiarvo parhaalle RIP-menetelmälle oli 0.71 ja IP-menetelmälle 0.53. RIP on tarkempi kuin IP, mutta RIP vaatii oman sensorin, kun taas IP voidaan mitata yhdenaikaisesti EKG:n kanssa samoista elektrodeista. Kehitetty signaalin laadun mittari paransi IP-menetelmän selitysastetta arvoon $R^2 = 0.66$. Tieto suhteellisesta hengitystilavuudesta menetetään potilaan asennon muutoksen myötä, mutta asennon muutos voidaan havaita muilla menetelmillä. Tulokset osoittavat, että IP ja RIP havaitsevat hengitystilavuuden suhteelliset muutokset.

Avainsanat:	Seuranta, Hengitystilavuus
Kieli:	Englanti

Contents

Abbreviations

BMI	body mass index
CO_2	carbon dioxide
ECG	electrocardiography
EIT	electrical impedance tomography
HR	heart rate
ICU	intensive care unit
IP	impedance pneumography
MV	minute-volume
PDM	patient data module
PPG	photoplethysmography
RIP	respiratory inductance plethysmography
RR	respiratory rate
SQI	signal quality index
SpO_2	peripheral capillary oxygen saturation
TV	tidal volume
ΔV	change in lung volume
ΔZ	change in electrical impedance

Chapter 1

Introduction

Traditional monitoring on hospital general care floors is based on a simple model where care personnel takes action when a physiologic parameter, such as peripheral capillary oxygen saturation (SpO_2), respiratory rate (RR) or heart rate (HR), is noticed having breached a predefined value. In modern hospitals, physiologic parameters are sampled from patients either continuously or intermittently in order to detect a change in patient condition [1].

RR is a routine vital sign tracked on patients, in addition to pulse rate, blood pressure, and temperature [2]. RR is an important measurement, change in which can predict serious events. Despite the importance, RR is the vital sign most frequently neglected [3].

While some studies have shown that a change in respiratory rate is a useful indicator of ventilatory depression, there is also evidence to suggest that it is not always that simple [1]. RR and the volume of air breathed in a one-minute period, minute-volume (MV), have been found weakly correlating [4], which means that RR alone is not a sufficient measure of ventilation of a patient. Thus, information about the volume would be relevant. Even a pulse oximetry monitor might not be capable of detecting patient deteoriation if the patient is provided with supplemental oxygen [5].

The instrument commonly used to measure breathing accurately is called a spirometer. Spirometer measures the flow of air coming from and going into the lungs. To measure the airflow accurately, however, it is required that the patient breathes through a facial mask. Also, spirometry is often used to spot-check the patient condition and not to perform long-term monitoring. A facial mask is a nuisance for a conscious patient because it disturbs talking, eating and drinking. Thus, for continuous monitoring, an indirect method would be more comfortable. There is recent interest for developing indirect respiration monitoring technology for both short-term spot-check [6] and long-term monitoring [7] purposes.

In this work, measurements for evaluating the feasibility of impedance pneumography (IP) and respiratory inductance plethysmography (RIP) for continuous respiratory volume monitoring were planned and performed. Algorithms for obtaining the minute-volume reading from signals were developed and compared with a simultaneous spirometry measurement. The scope of this thesis was to observe only the relative changes in the estimated minute-volume values. A setup where information about the patient posture would be available was considered. Furthermore, a signal quality index (SQI) was designed to evaluate if unreliable sections of the minute-volume readings could be detected from the data.

Chapter 2

Background

The respiratory and cardiovascular systems cooperate to supply oxygen and eliminate carbon dioxide from body cells. The respiratory system provides for gas exchange where oxygen diffuses from air into blood and carbon dioxide from blood to air towards lower concentrations. The cardiovascular system transports blood, that contains the gases, between the lungs and body cells [8]. Functionally, the respiratory system consists of the conducting zone that transports the air (nose, nasal cavity, pharynx, larynx, trachea, bronchi, bronchioles, and terminal bronchioles), and the respiratory zone where the gas exchange takes place (respiratory bronchioles, alveolar ducts, alveolar sacs, and alveoli). The respiratory system is presented in Figure 2.1.

Breathing movement is generated by contraction and relaxation of respiratory muscles, mainly the diaphragm. Muscle movement causes pressure inside the lungs to change. If the pressure in the lungs is higher than the atmospheric pressure, air flows out of the lungs, and vice versa. Continuous breathing is required to ensure that cells are fueled with oxygen and waste carbon dioxide is removed.

Respiratory effort is controlled in the brain by the respiratory center that transmits nerve impulses to the breathing muscles. Breathing can be voluntarily controlled to a certain degree. However, mainly the respiratory center reacts to changes in blood pH or partial pressure of carbon dioxide measured by chemoreceptors and adjusts the breathing effort accordingly.

The average RR of a healthy adult at rest is 12 breaths per minute and the average volume of one normal breath, tidal volume (TV), is 500 ml [8]. Average MV is thus 6 l. However, all air flowing through nose and mouth can not be utilized for gas exchange because of anatomical dead space. For a typical adult, about 70% of the tidal volume reaches the gas exchange zone. The volume of inhaled air that can be inspired in addition to the tidal volume is called inspiratory reserve volume. Correspondingly, the volume that can be exhaled after a normal expiration is the

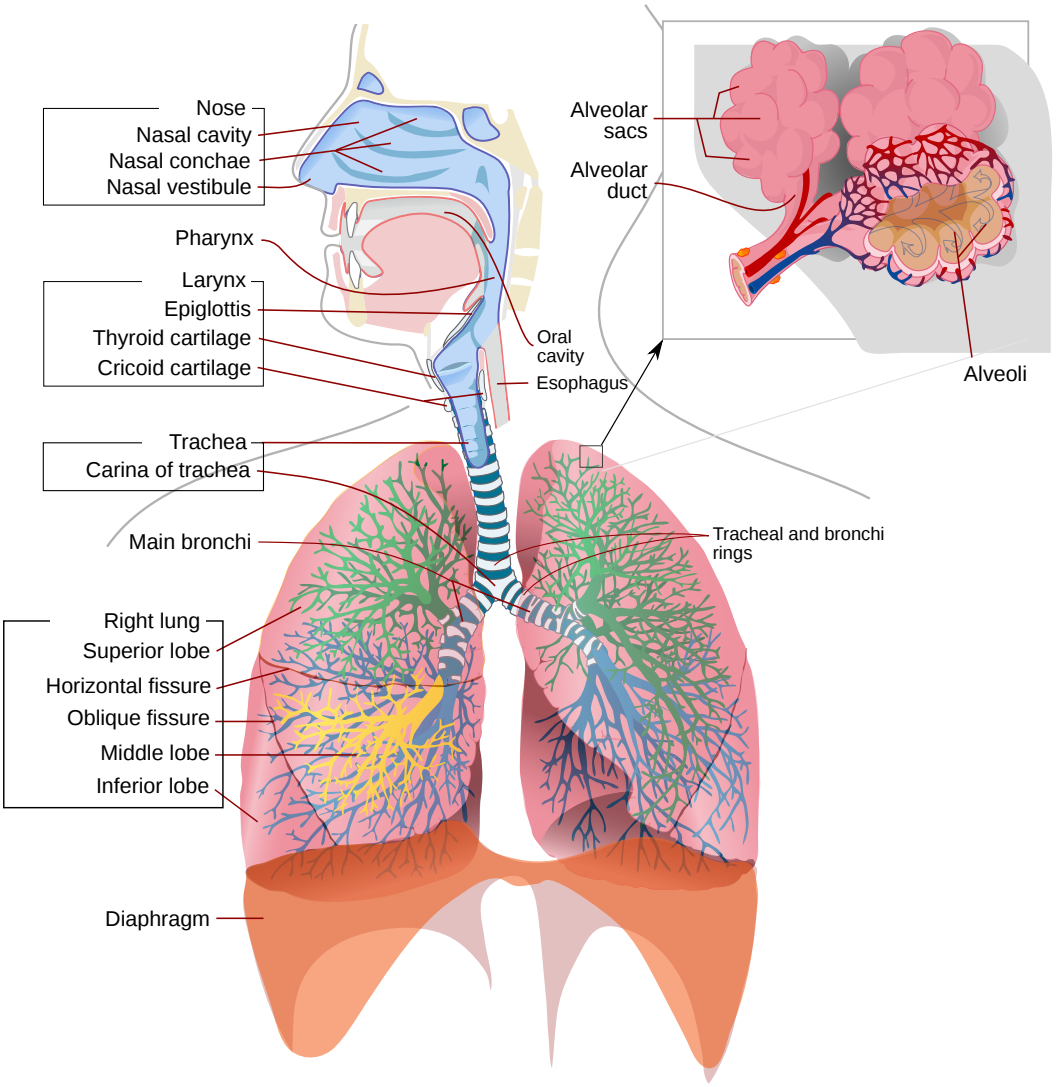

Figure 2.1: The respiratory system. Figure is modified from Wikimedia Commons [9].

expiratory reserve volume. The volume of the lungs after a maximal expiration is referred to as residual volume.

Possible problems with the respiratory system include blocking of the airway, impairment of the respiratory muscles (lack of signal from the brain or muscle failure), disruption of gas exchange or poor flow of blood from lungs to cells and back. Problems might be reacted with a change in RR or TV or both. Thus, a change in the breathing pattern may be the first sign of patient deterioration.

In obstructive apnea, breathing is ceased because of a block in the upper airway while breathing effort still exists. Central apnea occurs when breathing signal from the brain is missing. For patients with congestive heart failure, central sleep apnea has been correlated with male gender, atrial fibrillation, age and hypocapnia. However, for obstructive sleep apnea, only body mass index (BMI) increased risk for men and age for women [10]. Obstructive sleep apnea is present in a significant proportion of the population, but the majority of patients remain undiagnosed [11].

2.1 Respiratory monitoring

The gold-standard instrument used for measuring breathing volume is called a spirometer, which measures the flow of air coming from and going to the lungs. The principle of operation is to measure the airflow-generated differential pressure on the opposite sides of a small flow-resisting element [12]. Inspiratory and expiratory volumes can be obtained from the airflow values by integration. Spirometry, however, requires that the patient breaths through a facial mask, which is uncomfortable for a conscious patient since it disturbs talking, eating and drinking. Continuous spirometry measurement also requires relatively expensive instruments and trained care personnel usually available only in intensive care units. Thus, a reliable indirect method would be more feasible.

2.1.1 Impedance Pneumography

Electrical impedance pneumography (IP) is a widely used method for monitoring respiration noninvasively [13]. In IP, a weak high-frequency current (20–100 kHz, $\leq 100\ \mu$A) is injected into the tissue through the drive electrodes on the body. The current causes a potential difference to develop across any two points between the drive electrodes. This potential difference is related to the impedance of the tissue between the voltage-sensing or receive electrodes [14]. The high-frequency carrier signal is amplitude-modulated when passing the thorax. Measured voltage signal is then demodulated at the receiving side to extract the low-frequency breathing

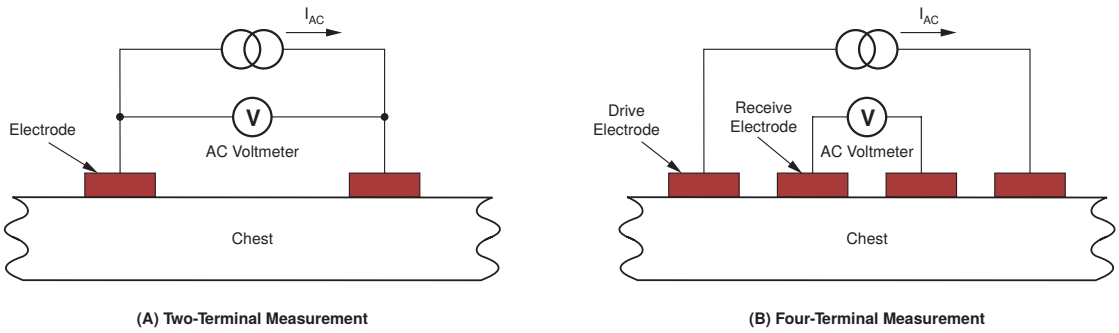

Figure 2.2: The diagrams of two-terminal and four-terminal IP measurements.

signal. Impedance respiration curve is the envelope of the measured high-frequency signal.

The measurement can be performed with four electrodes (four-terminal measurement) or using the same electrodes as both the driving and receiving electrodes (two-terminal measurement). In hospitals, the two-terminal measurement is preferred, since the measurement can be performed using existing ECG electrodes. However, the two-terminal measurement may have a non-linear voltage response due to current flowing through a polarization impedance at the electrode–tissue interfaces. The four- and two-terminal measurements are presented in Figure 2.2.

Electrical impedance is a measure of how much an object, such as human thorax, opposes the flow of electrical current through it. Electric current flow in transthoracic measurement is distributed into different types of tissue, and the exact mechanism behind the respiratory impedance signal is not known. However, literature suggests that lung tissue itself has a linear volume–impedance response [6]. The measured impedance signal contains also a contribution from other than the lung volume changes.

For lung volume measurements, ideally the relationship between the measured impedance change and lung volume change, $\frac{\Delta Z}{\Delta V}$ would be linear and constant. Absolute volume changes could be obtained after a calibration with a spirometer or with prior knowledge of the measurement sensitivity field and the tissue conductivities. Both options have been researched with varying results. Difficulties include the variations in human anatomy and uncertainties in determining the sensitivity field and tissue conductivities. Furthermore, the volume–impedance calibration may change with postural changes and even with patients in a static position due to, for instance, fluid accumulation [6].

Electrode location is an important factor in impedance measurements. For respiration measurements, electrode locations should be optimised so that cardiac and motion artefacts are minimized, and linearity and amplitude of $\frac{\Delta Z}{\Delta V}$ are maximized. A novel four-terminal electrode configuration for highly linear impedance-volume

relationship was recently reported [15]. The measurements were initially performed with standing test subjects, but later confirmed also in sitting and supine positions [16].

Initially, IP was used for recording respiratory volume [17]. Despite the efforts to improve accuracy of the measurement, multiple factors unrelated to the volume changes disturbed the volume determination too much. Such factors include cardiac artefacts, thoracic wall conductance, electrode instability, movement artefacts and signal amplitude changes with patient posture. Moreover, the reproducibility of impedance versus volume measurements within one person was poor, and variability from person-to-person was found high [18]. IP has been used as an apnea detector and as a RR monitor in hospitals. However, IP can not detect obstructive apnea reliably since the chest wall movement continues even if the airflow is blocked [19]. Nonetheless, TV monitoring using IP has been under development in the recent years [7, 15] since RR monitoring alone is not a sufficient measure of patient ventilation [4].

In addition to respiratory measurements, IP has been studied and used for measuring cardiac output, blood flow and body composition [20]. Electrical impedance tomography (EIT) is an imaging method based on similar impedance measurement. However, for image reconstruction, multiple electrode locations need to be used simultaneously.

2.1.2 Respiratory Inductance Plethysmography

Another method for measuring TV indirectly is respiratory inductance plethysmography (RIP). RIP is measured with an elastic band worn around the thorax. An electric wire wowen inside the band is the inductance element of a resonant electric circuit excited by AC-current. The inductance of the conductive loop is dependent on the cross sectional area enclosed, which changes with respiration. The change in inductance can be measured, for example, as a change in the circuit resonant frequency and thus information about the band deformation and breathing can be obtained [21].

Multiple bands can be used simultaneously to get a more complete description of respiratory motion. Typically, a rib cage and an abdominal band are used together resulting in TV measurement that correlates well with spirometry. It is claimed that RIP is the most accurate indirect TV measurement and that it is tolerant to patient movement [19]. However, there is evidence that, as IP, also RIP accuracy suffers from postural changes [22].

When using a rib cage and abdominal belts, obstructive apnea can be detected from the phase information of the belt signals. Upper airway obstruction introduces a phase difference to the signals that are normally in the same phase [23, 24]. There are even results that suggest that the degree of obstruction could be measured by

the RIP phase difference [25]. Thus, RIP is sometimes able to distinguish between central and obstructive apnea, unlike methods monitoring directly the respiratory gas movement. However, to accurately classify between central, obstructive and mixed apnea requires measuring the respiratory effort directly since movement may be minimal despite effort. Respiratory effort is most accurately measured by esophageal manometry [26].

RIP is used in sleep laboratories but also in hospital intensive care units (ICU) to noninvasively monitor ventilation. However, RIP is more expensive than IP so it is usually reserved for cases requiring more accuracy. Nonetheless, RIP has advantages over IP, including freedom from cardiac artefact and ability to detect obstructive apnea [27].

2.1.3 Other methods

There are also multiple other ways to obtain information about the respiration. Respiration rate monitoring instruments are usually based on measuring one of the following parameters: respiratory sounds, respiratory airflow, respiratory related chest or abdominal movements, respiratory CO_2 emission and oximetry probe SpO_2. Respiration rate can also be derived from the electrocardiogram (ECG) [28].

Airflow can be detected because exhaled air is warmer, has higher humidity and contains more CO_2 than inhaled air. These variations can be used for indicating the respiratory rate. Most airflow-sensing methods need a sensor attached to the airways. Sensors monitoring the airways can detect RR and apnea reliably compared to other methods [29]. However, the respiratory volume can not be determined because the thermistor, CO_2 and humidity sensors can only detect the direction of flow but not the magnitude. Monitoring the CO_2 level of air is called capnography and is considered the gold standard of respiratory rate measurement.

Sounds of breathing can be monitored with a microphone attached close to the respiratory airways or on the throat. The acoustic monitor is able to detect apnea but snoring, coughing, speaking, etc. can distort the measurement [28].

Respiration modulates heart beat intervals so that during inspiration beat-to-beat times are shorter than during expiration. The phenomenon is called respiration sinus arrhythmia [30]. Respiration signal can thus be obtained as far as the heart-beat timings can be determined, with e.g. pulse oximetry, ECG or accelerometers.

Pulse oximetry is based on the technique of photoplethysmography (PPG) where light transmitted through tissues is modulated by the blood flow pulse. In addition to variations in light modulation by the cardiac cycle, the PPG signal is also modulated by respiration [31].

In ECG, the electrical potential of the thorax is recorded at standardized locations with electrodes attached to skin. Not only does the respiration modulate

heart rate but also thorax geometry, which can be observed as the R-peak amplitude variation [32].

Respiration and other vital signs can also be detected by monitoring movement by non-contact methods, for example with radar technology [33] or a camera [34].

Chapter 3

Measurements

Two primary measurement sets, Set 1 and Set 2, were carried out for evaluating the feasibility of impedance pneumography and respiratory inductance plethysmography for respiratory volume monitoring. In total, 9 volunteers were measured in 15 sessions. Set 1 and Set 2 were measured with different test subjects. However, most of the test subjects were used in two sessions within a measurement set.

3.1 Measurement Protocol

In both sets, the test subjects were asked to breathe in certain ways, varying both the amplitude and the frequency of their breathing. In Set 1, the time of each breathing task was two minutes, and one minute in Set 2. The measurement protocol also included periods of simulated central apnea. About half of the protocol was measured while the test subject was lying on back and the other half while lying on either left side (Set 1) or right side (Set 2). The breathing instructions are presented in Table 3.1.

Breathing amplitude and breathing frequency were varied independently of each other. Predetermined quantitative values for the different levels of TV and RR were not given. The qualitative levels for TV were "shallow", "normal" and "deep" and for RR "low", "normal" and "high". Combination of "shallow" and "low" breathing was omitted to ensure that the test subjects would not start feeling uncomfortable due to insufficient oxygenation.

Duration of the central apnea periods was not predetermined. Instead, the test subject started breathing again when he/she wanted to. In most cases, though, the duration of apnea was more than 25 s.

Chest and stomach breathing were also recorded. In those tasks, the test subject was breathing so that only his/her chest or stomach was moving while the other

Table 3.1: Qualitative breathing instructions given to the test subjects. The protocol continued with the same set of instructions while lying on left side (Set 1) or right side (Set 2).

Task #	Position	Respiration rate	Breathing depth
1	back	normal	normal
2	back	apnea	apnea
3	back	normal	normal
4	back	low	normal
5	back	high	normal
6	back	high	shallow
7	back	normal	shallow
8	back	normal	deep
9	back	low	deep
10	back	high	deep
11	back	apnea	apnea
12	back	normal stomach	normal stomach
13	back	normal chest	normal chest
14	left/right	normal	normal
⋮	⋮	⋮	⋮

was kept static. Otherwise, in those tasks, the TV and RR were instructed to be "normal".

In Set 1, there was also a respiration "sweep" measurement at the end of each measurement. In "sweep"-task, the test subject started breathing with high TV and low RR gradually decreasing the volume and increasing the frequency.

Beginning and end times for each breathing task were written down to a xlsx-file together with other notes and patient information.

3.2 Measurement devices

In both sets, a CARESCAPE patient monitor was used with a CARESCAPE respiratory module and CARECSAPE patient data module (PDM). The CARESCAPE product family is designed and manufactured by GE Healthcare (Chicago, Illinois, the United States). The monitor was connected to a laptop that had S5 Collect software (GE Healthcare) installed. S5 Collect was used to record various physiological signal waveforms and trends measured by the monitoring system. The CARESCAPE-recorded signals used in this work were ECG (PDM), impedance respiration (PDM) and airflow (respiratory module) through a face mask. The impedance signal was recorded at 60-Hz and airflow at 25-Hz sampling frequency.

Measured ECG signals varied between sessions. Impedance was measured using a two-terminal configuration between right arm (RA) and left leg (LL) ECG electrodes, which is lead II in the standard 12-lead ECG configuration.

RIP was recorded with Embla titanium (Natus Medical Incorporated, Pleasanton, California, the United States) in both measurement sets. Two RIP belts (XactTrace single use cut-to-fit Embla RIP belt, Natus Medical Incorporated) were used to record the movement of thorax at rib cage and abdominal levels. The two RIP-signals were recorded at 32-Hz sampling frequency and then transferred to a computer for further analysis via USB-connection using the RemLogic software (Natus Medical Incorporated).

A prototype device developed in Riga Technical University in Latvia was used in Set 2. The system measured resistance of four stretch sensors knitted horizontally onto a t-shirt [35]. Topmost sensor was at axilla level and the bottom one below umbilicus. Height of each sensor ribbon was approximately 5 cm and they were equally spaced. Backside of the shirt did not have sensor ribbon and resistance of each ribbon was measured between left and right lateral. Resistivity sampling rate was 128 Hz and values the were sent to a custom-made LabVIEW-software via a Bluetooth-connection.

The 5-lead ECG electrode placement is presented in Figure 3.1. The four stretch sensors of the t-shirt system are marked with yellow colour. The Embla system band locations correspond approximately to the first and third yellow strip counted from the top.

3.3 Measurement Set 1

Ten measurements were performed using six test subjects. Four subjects were recorded twice. The measurements and synchronization of signals for measurement Set 1 were performed outside of this work at VTT Tampere.

Four test subjects were male and two female, age between 28 and 52 years, height from 166 to 192 cm and weight from 66 to 92 kg.

The duration of breathing tasks was two minutes and the latter half of the measurement was done while the patient was lying on his/her left side. The "sweep" task at the very end of the measurement was in V64 done while the test subject was lying on left side, but otherwise the subjects were lying on their back during that task.

A CARESCAPE B450 patient monitor was used. In one measurement session lead I, II and III ECG were recorded with 300-Hz sampling frequency due to a problem with the data connection. Otherwise, 5-lead ECG was recorded in all measurements with 500-Hz sampling rate. Electrode placement for 5-lead ECG is illustrated in Figure 3.1.

Multiple other measurement devices were also connected to the patient during the measurements, but only ECG, RIP, impedance respiration and airflow data were used in this work. Set 1 measurement IDs start with letter "V" in Table 3.2.

3.4 Measurement Set 2

Measurement Set 2 was taken in GE Healthcare Finland premises in Helsinki as part of this thesis. Data were collected in five measurement sessions with three volunteers (2 male, 1 female, between 30 and 65 years old, between 170 and 190 cm in height and weight from 60 to 85 kg). Two volunteers were measured twice.

The breathing tasks were similar to those used in Set 1. However, the duration of tasks was one minute and in the latter half of the measurement session, test subjects were lying on their right side. The latter half of the protocol was omitted in L5 and L6 due to lack of time. The sweep task at the end of measurement protocol was not included in Set 2 measurements.

Data was recorded simultaneously with three systems: CARESCAPE B650, Embla titanium RIP belts and the t-shirt prototype device. Embla system was the same that was used also in measurement Set 1. In addition to the impedance respiration and airflow measurements, single lead ECG (lead I) with 300-Hz sampling rate was recorded with the CARESCAPE patient monitor. Set 2 measurement IDs begin with letter "L" in Table 3.2.

Table 3.2: The recorded signals in the measurements. The numbers in signal-rows are sampling frequencies of the signals. Set 1 measurements have ID's starting with letter "V" and measurement Set 2 ID's start with "L". Test subjects are identified in the bottom by a number. Some test subjects were measured twice.

Measurement ID	V60	V61	V62	V63	V64	V70	V72	V73	V74	V75	L1	L3	L4	L5	L6
Airflow	25	25	25	25	25	25	25	25	25	25	25	25	25	25	25
Impedance Respiration	60	60	60	60	60	60	60	60	60	60	60	60	60	60	60
Embla 1, 2	32	32	-	32	32	32	32	32	32	32	32	32	32	32	32
T-shirt 1, 2, 3, 4	-	-	-	-	-	-	-	-	-	-	128	128	128	128	128
5-lead ECG	-	500	500	500	500	500	500	500	500	500	-	-	-	-	-
Lead I, II, III ECG	300	-	-	-	-	-	-	-	-	-	-	-	-	-	-
Lead I ECG	-	-	-	-	-	-	-	-	-	-	300	300	300	300	300
Test subject ID	0	1	2	3	4	0	2	3	4	5	6	7	8	8	7

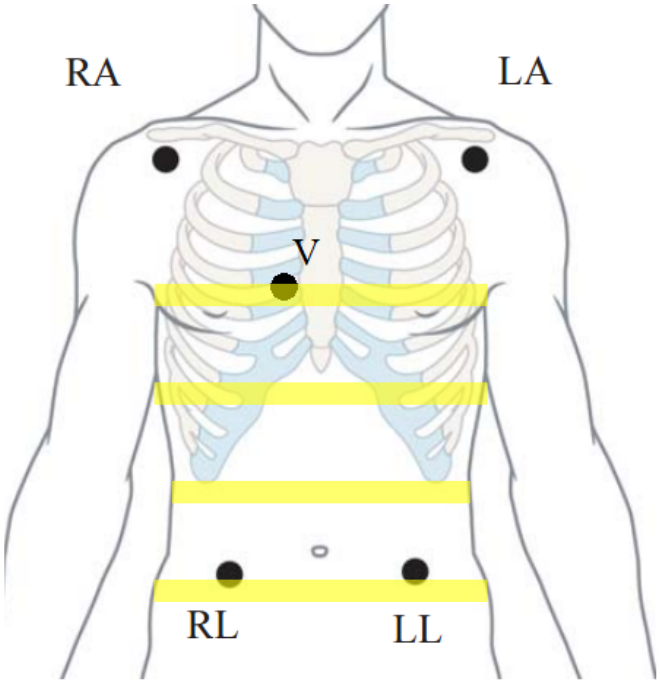

Figure 3.1: 5-lead ECG electrode locations together with the t-shirt system stretch belt sensor placement. Embla sensors were located approximately on top of the topmost and the third t-shirt belts.

Chapter 4

Analysis

Physiological signals were collected in 15 measurement sessions with nine voluntary test subjects. During the measurement sessions, test subjects performed breathing tasks varying the frequency and amplitude of breathing.

The signals were analysed with MATLAB software (The MathWorks, Inc, Natick, Massachusetts, the United States) version R2015b for 32bit Windows. 12 estimation methods were defined and ran to produce minute-volume values from the measured signals. Coefficient of determination between the minute-volume from an estimation method and the reference method was determined for each measurement session to assess whether the estimation method would be suitable for monitoring minute-volume continuously.

The data recorded by different systems — each having its own clock — was synchronized with each other and the breathing task timings after the measurements. Measurement Set 1 synchronization was done outside of this work at VTT Tampere. Measurement Set 2 signals were synchronized manually with MATLAB software by matching the endpoints of apnea breathing tasks. Artefacts were created in the data in the beginning and end of each measurement to help the synchronization process but they were not clear enough so the periods of apnea were used for synchronization instead. The achieved accuracy in synchronization was approximately two seconds, which is within one normal breath.

4.1 Preprocessing of signals

The impedance and ECG signals measured by PDM were already high-pass filtered by the recording hardware. In two evaluated processes, the impedance signal was further filtered with QRS complex timings determined from the ECG signal. This filter was adaptive to both the time between QRS complexes and the shape of the cardiogenic oscillations. The adaptive filtering suppressed the cardiogenic

oscillations in the impedance signal. However, if the breathing rate and heart rate were approximately equal, the breathing signal was interpreted as cardiogenic oscillation and was filtered out. The QRS complex timings were determined by an algorithm developed outside of this work. Output of the QRS timing algorithm was compared with raw signals to visually verify that the timings were reasonable.

Signals recorded by Embla RIP belt system were also already high-pass filtered by the recording hardware. Embla signals were not preprocessed further in the processes but were passed on for volume calculations.

T-shirt system did not have any embedded filtering and the signals were not preprocessed in any way. Raw signals had large DC-offset but they were passed on directly for volume calculations.

4.2 Volume calculation algorithm

Tidal volumes were determined by searching the local minima and maxima of each recorded signal with a few conditions. In the first step of the algorithm, if a sample was greater than all other samples in its one-second neighbourhood, it was marked as a local maximum. The local minima were searched in a corresponding way. From the marked values, the minimum value before the first maximum value – the minimum of local minima – was considered the start of first breath. Then, the greatest of the maxima between the first and second minimum was marked as the point of maximum lung volume. This marking procedure was continued for marked minima and maxima until the end of the signal to obtain an alternating sequence of minimum and maximum values.

The marked minima were now considered as the beginning and the end points of breaths and the maxima as instants of maximum lung volume. Thus, each breath consisted of a start, a maximum and an end value, from which the tidal volumes were determined. The inspiratory tidal volume was the difference between the start and maximum values and expiratory tidal volume the difference between the maximum and end values. An example of the peak searching and marking algorithm is presented in Figure 4.1.

Minute-volume was determined from the tidal volume values of the previous one-minute period. Structure resembling a ring buffer was used. Individual breaths were added to a one-minute long moving buffer only if the combined duration of breaths inside the buffer would be less than one minute. A breath was also removed from the buffer if it did not fit in entirely. Minute-volume was then calculated by summing all tidal volumes in the buffer and dividing by the total duration of the breaths in the buffer, which may be less than one minute. Separate values for inspiratory and expiratory minute-volumes were calculated, but only expiratory minute-volume was used for analysis. The minute-volume value was updated every

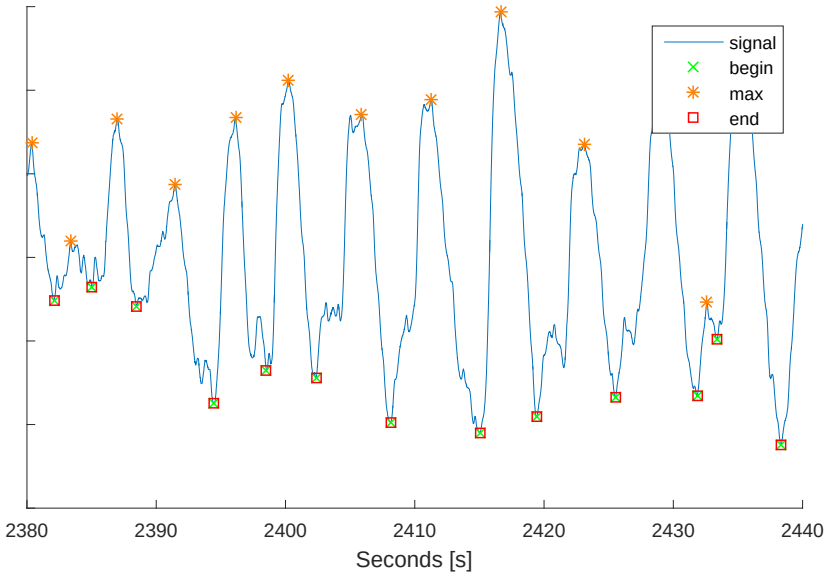

Figure 4.1: Output of the peak search algorithm. The beginning, maximum and endpoints of each breath are marked and used for tidal volume calculations.

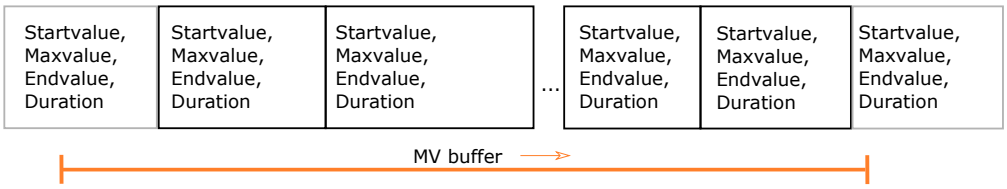

Figure 4.2: Minute-volume buffer diagram. Grey boxes represent breaths not included in the buffer. TV of a breath was determined from the start-, maximum- and endvalue. Minute-volume was then determined from the TVs and breath durations.

time the buffer is updated, i.e. when new breath was added or an old breath was removed from the buffer. Minute-volume buffer window is illustrated in Figure 4.2.

Reference value for minute-volume was obtained from the airflow signal. The measured airflow was integrated to obtain the instantaneous lung volume. From the real-time lung volume signal, the tidal and minute-volumes were calculated similarly to the other signals.

4.3 Estimation methods

The measured signals were used to determine minute-volume of breathing in various ways, called estimation methods. Total of 12 different estimation methods were evaluated. In principle, in all estimation methods MV was calculated by determining the signal amplitude in the same way. However, the signal sources were different and multiple signals were combined in three of the 12 estimation methods. For combining signals, two estimation methods used the mean of individual MVs and one estimation method the median. The combined estimation methods used signals measured by either the t-shirt prototype or Embla system. Different Embla or t-shirt signals were assumed to have same scaling, thus giving similar contribution to minute-volume. All estimation methods evaluated in this work are described in Table 4.1.

The scope of this thesis was to evaluate only the relative changes in MV i.e. not to convert and calibrate the obtained values into units of volume. For visual inspection, though, MV curves were matched at a calibration point chosen at the beginning of the measurement when the test subject had been breathing normally for at least a minute.

Measurement-wise coefficients of determination were calculated for each process. Two linear regression models were fitted to the MV readings at the endpoints of breathing tasks. MV of the reference method was used as the dependent variable. In Model 2, only the measured MV value of each process was used as the independent variable. In Model 1, also the test subject posture information was used as an independent variable. Model 1 is illustrated in Equation (4.1) and Model 2 in Equation (4.2). Models were fitted using the least squares method.

$$y_i = \beta_0 + \beta_1 x_{i1} + \beta_2 x_{i2} + \beta_3 x_{i1} x_{i2} + \varepsilon_i \tag{4.1}$$

$$y_i = \beta_0' + \beta_1' x_{i1} + \varepsilon_i', \tag{4.2}$$

where subscript i refers to the endpoint of breathing task number i, y is the MV of the reference process, x_{i1} is MV reading of a process being evaluated, x_{i2} is a binary dummy variable indicating the position and ε_i is the residual minute-volume. Coefficient of determination, R^2, was obtained by

$$R^2 = 1 - \frac{\sum_i (y_i - \hat{y}_i)^2}{\sum_i (y_i - \overline{y})^2}, \tag{4.3}$$

where $\hat{y}_i$ is the MV value at point i predicted by the obtained model parameters and $\overline{y}$ is mean value of the observed reference values y_i.

4.4 Postprocessing

For all processes that did not combine multiple measured signals, a signal quality index (SQI) was calculated. It was used to invalidate the obtained MV readings. SQI at a given instant was calculated from the measured signal in the previous one-minute period and MV reading was invalidated if the SQI did not reach a required threshold. Different values for threshold were used to quantify the trade-off between R^2 and the invalid time of the MV reading.

The idea of the SQI algorithm was to evaluate the amount of periodicity in the signal. First, the signal was resampled to 10 Hz frequency and 15-s moving average was removed. Then, correlation Q of 15-s period with the previous 45-s period was evaluated,

$$Q(t,t') = \frac{\int_0^{15\text{ s}} dt''\ \left(s(t-t'') - s(t'-t'')\right)^2}{\int_0^{15\text{ s}} dt''\ s(t'-t'')^2}, \tag{4.4}$$

where $s(t)$ is the measured signal at time t and t' is the amount of lag. $Q(t,t')$ was evaluated for all t and $t - 30\text{ s} < t' < t - 3\text{ s}$. If correlation above the threshold value existed with more than three second lag, the signal state of that point was high,

$$S'(t) = \begin{cases} 1, & \text{if } Q(t,t') > T \text{ for any } t - 30\text{ s} < t' < t - 3\text{ s} \\ 0, & \text{otherwise} \end{cases}, \tag{4.5}$$

where T is the threshold value. Threshold values T ranged from 0.3 to 1 with 0.1 interval. To make the signal state, $S'(t)$, more stable, requirement was that the state had to be stable for 5 seconds before it was changed. The final step was to look at the obtained value for one minute and if the signal state had been high for at least 30 seconds during that minute, the final SQI of the point was high:

$$SQI(t) = \begin{cases} 1, & \text{if } \dfrac{\int_{t-60\text{ s}}^{t} dt'\ S(t')}{60\text{ s}} > \frac{1}{2} \\ 0, & \text{otherwise} \end{cases}. \tag{4.6}$$

A diagram of the SQI calculation process is presented in Figure 4.3. Flowchart of the whole analysis process is shown in Figure 4.4.

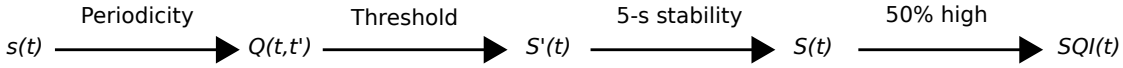

Figure 4.3: Diagram of the SQI algorithm workflow.

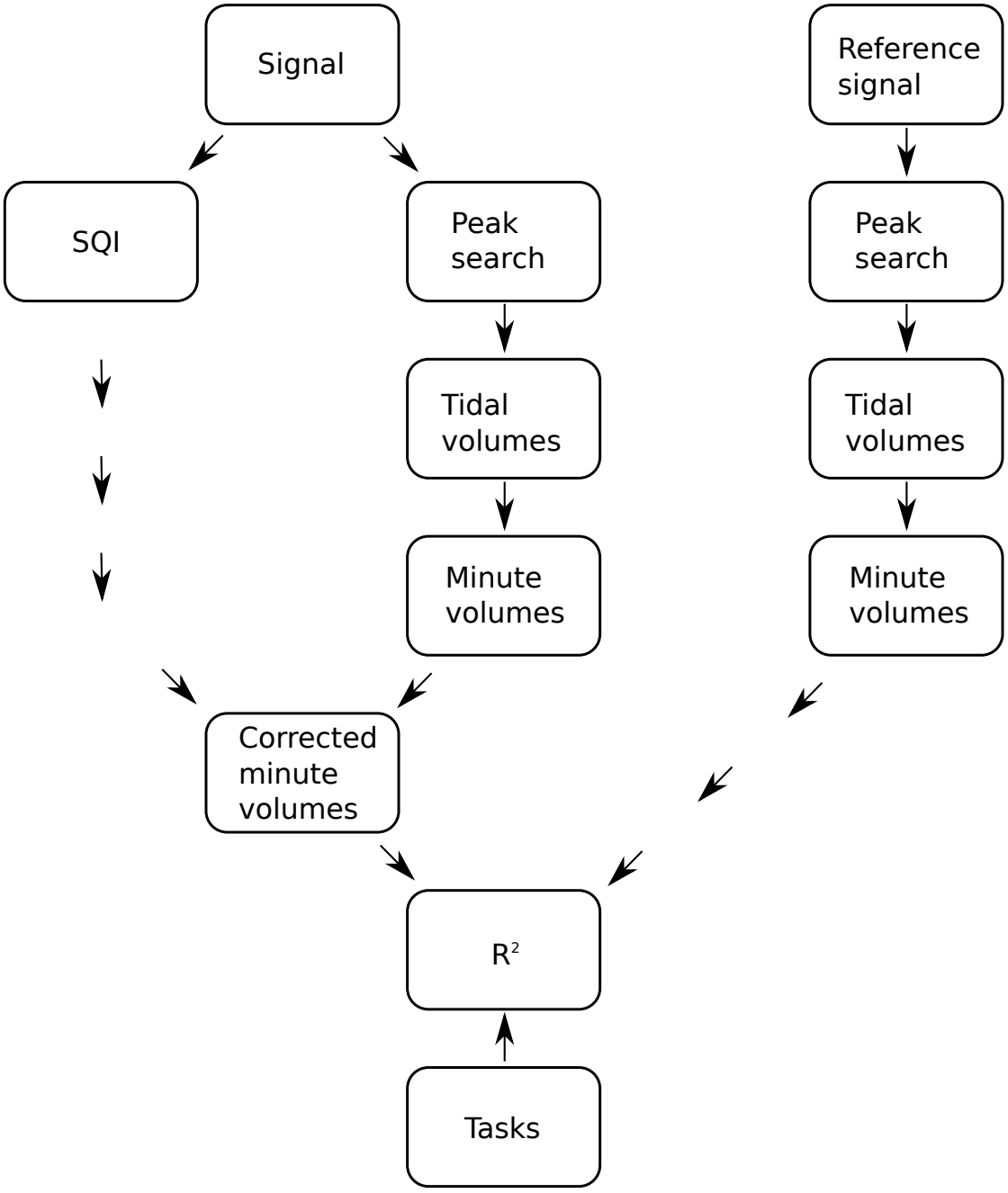

Figure 4.4: Flowchart of the analysis process.

Table 4.1: Evaluation methods used in this work.

#	**Process name**	**Signal source**	**Steps**
1	Embla peaks average :: embla1	embla 1	TV from peak search, 60s MV window
2	Embla peaks average :: embla2	embla 2	TV from peak search, 60s MV window
3	Embla MV fusion peaks average	embla 1, embla 2	For each signal: TV from peak search, 60s MV window. Combine MV curves by taking mean
4	Resp raw peaks average	Impedance respiration	TV from peak search, 60s MV window
5	Resp peaks average	Impedance respiration, ECG	Cardiac artefact filtering, TV from peak search, 60s MV window
6	Resp peaks average middle	Impedance respiration, ECG	Cardiac artefact filtering, TV from peak search, 70s median MV window
7	tshirt peaks average :: tshirt1	t-shirt 1	TV from peak search, 60s MV window
8	tshirt peaks average :: tshirt2	t-shirt 2	TV from peak search, 60s MV window
9	tshirt peaks average :: tshirt3	t-shirt 3	TV from peak search, 60s MV window
10	tshirt peaks average :: tshirt4	t-shirt 4	TV from peak search, 60s MV window
11	tshirt MV mean peaks average	t-shirt 1, t-shirt 2, t-shirt 3, t-shirt 4	For each signal: TV from peak search, 60s MV window. Combine MV curves by taking mean
12	tshirt MV median peaks average	t-shirt 1, t-shirt 2, t-shirt 3, t-shirt 4	For each signal: TV from peak search, 60s MV window. Combine MV curves by taking median

Chapter 5

Results

15 measurement sessions were performed with voluntary test subjects. The test subjects varied both the amplitude and the frequency of breathing according to a test protocol shown in Table 3.1. Measured signals for each measurement session are shown in Table 3.2.

A few measurements were omitted from the analysis after an initial inspection of the signals. In V61, the impedance respiration signal scaling changed to an unknown value during the measurement. The scale change was visible after the cardiac artefact estimation algorithm. In measurements V64, V74 and V75 the dynamic range of the impedance measurement was not large enough to capture the whole signal and, as a result, the signal amplitude was capped. Measurements V61, V64, V74 and V75 were thus omitted since the analysis was based on observing the changes in signal amplitude.

Also the airflow signal had invalid values in six of the 11 analysed measurements. Reference minute-volume values affected by the invalid airflow signal were invalidated and excluded from the analysis. The invalid values were related to a strong breath before or after apnea or the "high RR, deep breathing"-task. Maximum of two points were left out of the regression model fits due to invalid airflow signal in any measurement session.

Coefficients of determination, R^2, were calculated for 12 processes described in Table 4.1. Minute-volume calculated from the airflow signal was used as the reference value, i.e. dependent variable. Two regression models were fitted: Model 1 and Model 2. Both models used MV of evaluation method as an independent variable and Model 1 used test subject posture information as an additional independent variable. Model 1 and 2 equations are presented in Equations (4.1) and (4.2), respectively. MV values were fitted to values at the end of each task. R^2 values of Model 1 are presented in Table 5.1 and in Table 5.2 for Model 2.

Model 1 fit is missing from measurements L5 and L6, because only first half of the protocol was performed. Furthermore, Embla system was not used in measure-

ment V62. Average R^2 column is calculated directly from the shown R^2 values for each measurement, i.e. the unweighed average. The results are sorted to descending average R^2 and no SQI was used for the results in these tables.

In measurement V60, Model 1 has much higher R^2 value than Model 2, which means that changing posture also changed the amplitude of the signal the MV was determined from. The same test subject was measured also in V70, where similar change does not occur.

Impedance respiration evaluation methods have more intermeasurement variation than the Embla processes. The highest scores of impedance evaluation methods are comparable to Embla but R^2s for especially V63 and V72 are particularly low.

There is variation also in Embla evaluation methods' scores. However, using both RIP-belts improves worst-case scores and, in most cases, results in higher R^2 than either of the belts alone. On average the abdominal RIP-belt, "embla 2", scores higher than the "embla 1" belt at axilla level.

The third stretch belt, "tshirt 3", performed better than the other ones. That belt was placed approximately at the same level as the bottom Embla RIP-belt, "embla 2". For t-shirt signals, there is no as much benefit from combining the minute-volumes as with Embla by simply taking the mean or median value.

In further analysis, the developed SQI method was used to invalidate MV values in order to evaluate if the R^2 values could be increased. The SQI was used only for evaluation methods that did not combine minute-volume curves, and only for fitting regression Model 2. Average results for measurement Set 1 are shown in Figure 5.1 and for Set 2 in Figure 5.2.

For Set 1 measurements, R^2 of impedance evaluation methods is improved when the threshold value in SQI algorithm is increased and more data is disregarded. However, the opposite happens for Embla evaluation methods. The effect is not observed with measurement Set 2, though, where all results improve slightly as the condition on periodicity tightens.

The proportion of invalidated data as a function of respiration amplitude for "Embla peaks average :: embla2" and "Resp raw peaks average" is shown in Figure 5.3. The proportion of invalidated data is inversely proportional to the breathing amplitude and stomach breathing is invalidated more often than chest breathing.

Minute-volume curves of "Resp raw peaks average", "Embla peaks average :: embla2" and "Embla MV fusion peaks average" for V70 are presented in Figure 5.4. The minute-volumes are shown both before and after the SQI algorithm invalidation step. Grey boxes are the breathing tasks, and movement artefacts caused by posture changes can be seen as peaks in MV determined by the "Resp raw peaks average" process. MV curves are scaled so that the readings at the end of the third

Table 5.1: Coefficients of determination, R^2, of Model 1 fitting to MV curves. Model 1 uses both the MV determined by evaluation method and the posture information as independent variables, as shown in Equation (4.1). SQI was not used for these results. Evaluation methods are sorted by average R^2 column.

	model1									
Evaluation method	V60	V62	V63	V70	V72	V73	L1	L3	L4	average
Embla MV fusion peaks average	0.89		0.77	0.77	0.45	0.82	0.87	0.52	0.59	0.71
Embla peaks average :: embla2	0.78		0.75	0.69	0.61	0.74	0.66	0.45	0.21	0.61
tshirt peaks average :: tshirt3							0.81	0.09	0.70	0.53
Resp raw peaks average	0.76	0.34	0.10	0.61	0.13	0.64	0.88	0.59	0.73	0.53
Embla peaks average :: embla1	0.79		0.20	0.55	0.24	0.56	0.87	0.11	0.73	0.51
Resp peaks average middle	0.73	0.27	0.05	0.57	0.13	0.55	0.83	0.64	0.75	0.50
tshirt MV mean peaks average							0.80	0.18	0.50	0.49
tshirt MV median peaks average							0.76	0.21	0.47	0.48
Resp peaks average	0.74	0.21	0.03	0.50	0.07	0.51	0.83	0.61	0.73	0.47
tshirt peaks average :: tshirt2							0.67	0.17	0.37	0.41
tshirt peaks average :: tshirt4							0.75	0.05	0.41	0.41
tshirt peaks average :: tshirt1							0.60	0.17	0.37	0.38

Table 5.2: Coefficients of determination, R^2, of Model 2 fitting to MV curves. Model 2 uses only the MV determined by evaluation method as an independent variable, as shown in Equation (4.2). SQI was not used for these results. Evaluation methods are sorted by average R^2 column.

	model2											
Evaluation method	V60	V62	V63	V70	V72	V73	L1	L3	L4	L5	L6	average
Embla MV fusion peaks average	0.32		0.68	0.73	0.42	0.77	0.85	0.51	0.54	0.78	0.84	0.64
tshirt peaks average :: tshirt3							0.70	0.07	0.63	0.80	0.62	0.56
tshirt MV mean peaks average							0.64	0.07	0.48	0.79	0.73	0.54
tshirt MV median peaks average							0.57	0.10	0.46	0.82	0.75	0.54
Embla peaks average :: embla2	0.24		0.70	0.67	0.48	0.65	0.65	0.38	0.16	0.48	0.77	0.52
tshirt peaks average :: tshirt4							0.74	0.03	0.40	0.68	0.64	0.50
Resp raw peaks average	0.44	0.33	0.06	0.47	0.13	0.54	0.80	0.25	0.65	0.95	0.48	0.46
Resp peaks average middle	0.43	0.27	0.04	0.56	0.13	0.46	0.78	0.23	0.64	0.40	0.75	0.43
tshirt peaks average :: tshirt1							0.33	0.07	0.33	0.74	0.60	0.41
Embla peaks average :: embla1	0.26		0.18	0.38	0.24	0.51	0.85	0.01	0.72	0.66	0.20	0.40
Resp peaks average	0.41	0.21	0.00	0.45	0.07	0.44	0.76	0.29	0.63	0.42	0.48	0.38
tshirt peaks average :: tshirt2							0.44	0.07	0.33	0.82	0.14	0.36

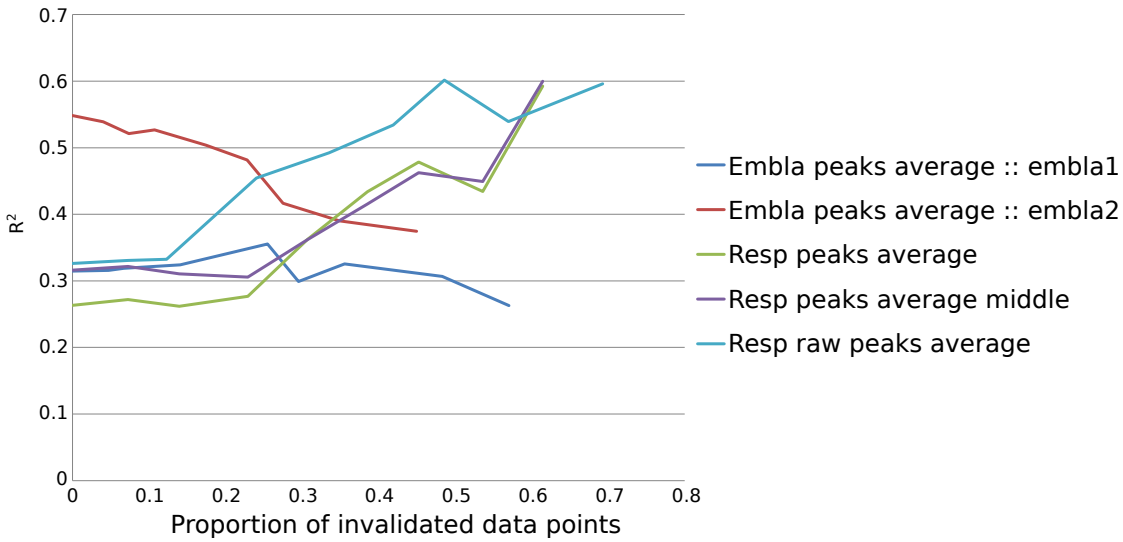

Figure 5.1: R^2 as a function of proportion of fitting points left out by SQI method for Set 1 measurements when Model 2 was fitted. Impedance respiration results improved but Embla degraded as threshold condition was tightened.

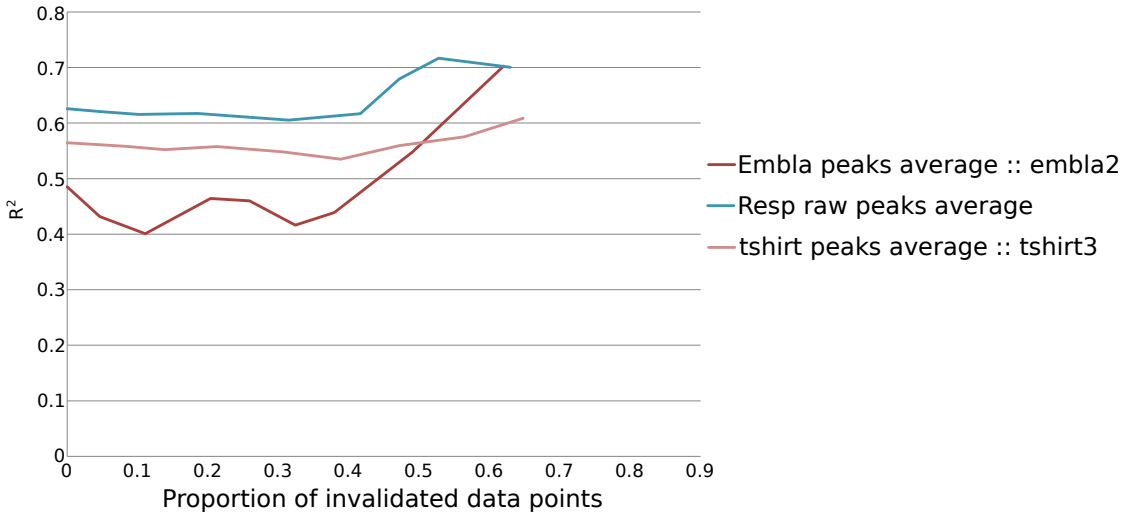

Figure 5.2: R^2 as a function of proportion of fitting points left out by SQI method for Set 2 measurements when Model 2 was fitted. Results improved slightly as the threshold condition was tightened.

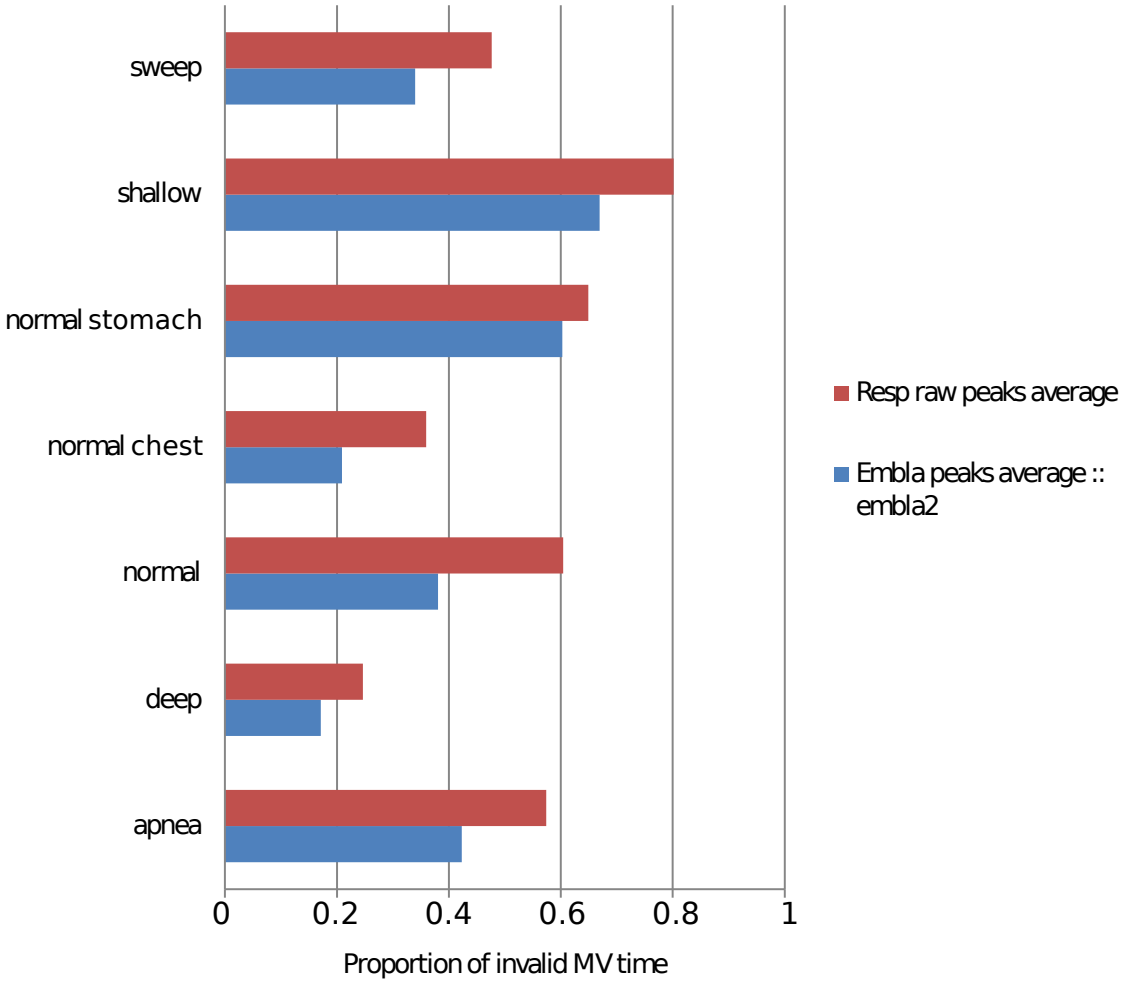

Figure 5.3: Proportion of time the SQI algorithm invalidated MV values for two selected processes with threshold value $T = 0.5$. More data was invalidated when test subjects were breathing with their stomach than when breathing with their chest and amount of invalidated data increased as breathing amplitude decreased. With the same threshold condition, impedance signal was rejected more often than the Embla signal.

task are matched. Even when the minute-volume readings were invalidated, they were reasonable at least most of the time.

Median tidal volumes of the same breaths are plotted in Figure 5.5. The curves are scaled also so that they match at the end of the third breathing task. Tidal volume from the Embla signal follows the spirometry tidal volume well throughout the measurement. Tidal volume from the impedance signal is not accurate when the test subject is lying on left side or the breathing is slow and deep. The median volume depends on how well the detected individual breaths match from different signals. The spirometry volume and Embla signals are smoother compared to the raw impedance signal. The spikiness of impedance results in more minima and maxima points especially with slow breathing. Moreover, the spikiness is increased when the test subject is lying on side.

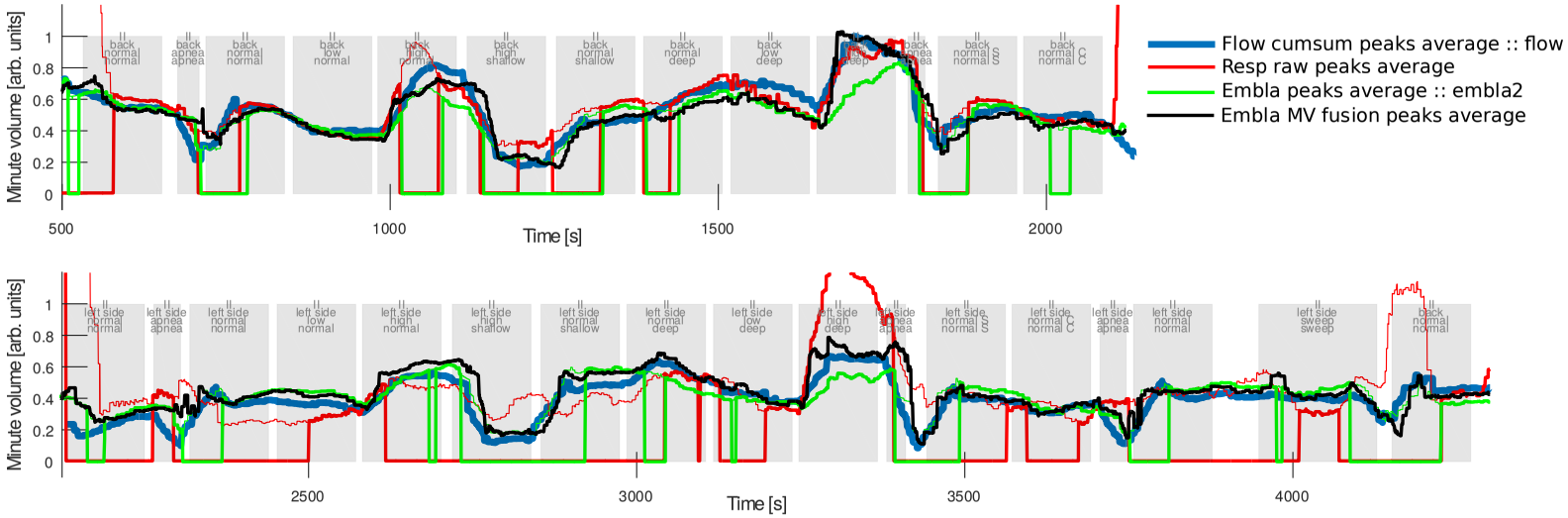

Figure 5.4: Selected MV signals for V70. Grey boxes are the breathing tasks. SQI algorithm was not used for "Embla MV fusion peaks average", but results for the two other processes are shown both with and without the SQI invalidation ($T = 0.5$). R^2 for "Resp raw peaks average" improved from 0.47 to 0.67 with SQI and for "Embla peaks average :: embla2" from 0.67 to 0.70. Out of the 30 fitting points, SQI algorithm invalidated 12 points from "Resp raw peaks average" measurement and 5 points from "Embla peaks average :: embla2". R^2 of "Embla MV fusion peaks average" is 0.73.

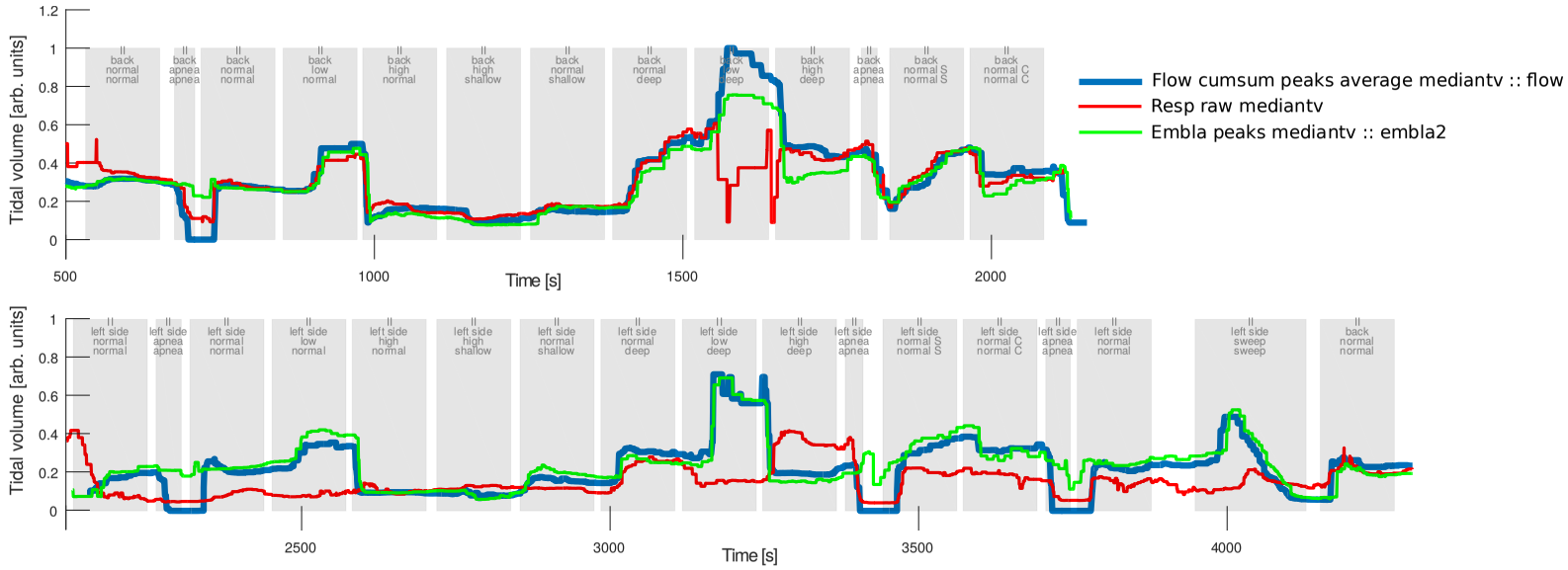

Figure 5.5: Median tidal volume plots of processes "Resp raw peaks average" and "Embla peaks average :: embla2" for measurement V70. Grey boxes represent the breathing tasks. Tidal volume from Embla signal follows the spirometry tidal volume well throughout the measurement. Tidal volume from the impedance signal is not very accurate when the test subject is lying on left side.

Chapter 6

Discussion

The goal of this work was to evaluate the feasibility of indirect measurements for respiratory volume monitoring. 15 measurement sessions were performed with nine voluntary test subjects, who varied both the amplitude and frequency of their breathing. Coefficients of determination, R^2, were calculated for 12 evaluation methods. Minute-volume calculated from the airflow signal was used as the reference value. We considered a setup where posture information is available from other sensors. Thus, in addition to minute-volume from the evaluation method, regression Model 1 used test subject posture as an additional independent variable. The developed periodicity-based SQI algorithm was then used to invalidate minute-volume values and observe the effect on R^2.

Overall, "Embla MV fusion peaks average" had the best performance measured by average, best worst case and least variance. Next come other Embla processes with the t-shirt ones. T-shirt processes do not benefit from combining signals as much as Embla processes, maybe because the worst t-shirt processes are often worse than the worst Embla processes. However, t-shirt processes also suffer from small sample size, especially for Model 1.

The impedance process "Resp raw peaks average" result is better than other impedance processes where cardiac artefact was filtered from the signal. The adaptive filtering removes some of the high RR breathing, which impedes the performance.

However, only healthy volunteers were measured, not real patients in hospital environment. The breathing protocol was designed to include multiple types of breathing and was not based on any data. Hospital test data would be required to see the results in a real sample of breathing with actual patients.

In Set 1 measurements, multiple other measurement devices were also connected to the test subjects. No disturbance from the other devices was visible in the data. However, they may have disturbed the patient during the measurement,

i.e. the data might have been different if the devices unused in this work had been left out.

Fitting points of minute-volume curves were taken from the end of each breathing task, where the breathing and therefore minute-volume were assumed to have been stabilized. Synchronization of signals and tasks was thus not thought to be very critical for overall results even though apnea task duration was in most cases less than one minute and Set 1 measurements had the "sweep"-task at the end. Synchrony was checked visually for all signals in all measurements.

PDM high-pass-filtered the ECG and impedance signals. Impedance signal was somewhat distorted compared to the volume signal but the amplitude was reasonable as shown by the results for minute-volume. Furthermore, the patient monitor can change impedance signal scaling to an unknown value even if the scaling is set manually. V61 was omitted because of the changed scaling.

In these measurements, IP was measured only from ECG lead II. Using existing ECG electrode locations does not require extra effort from the care personnel in hospitals. However, other electrode locations should be studied if accuracy improvements are wanted.

In measurements V64, V74 and V75 the impedance signal amplitude was capped. It could be speculated that the capping of the impedance signal was due to thinness of the test subject, but similar capping happened also with test Subject 5, who had a body mass index (BMI) similar to those subjects with whom capping did not occur. Test Subject 4 had lower BMI than the other test subjects but, however, it was within the normal range between 20 and 25. Signal capping is not a problem in more recent devices where DC-measurement is performed with more dynamic range and measurement resolution.

Minute-volume is not always poor when SQI invalidates the result. SQI was based on signal periodicity. The periodicity might not the optimal way to evaluate quality of signals since the breathing itself can be irregular.

Results with SQI for Set 2 measurements may be overly affected by the shortness of breathing tasks. SQI has one minute delay so that tasks where lots of minute-volume readings were disregarded might also correlate with the previous task. Measurement Set 2 also has a small sample size and therefore is sensitive to outliers in results.

Previous research has found that the signal amplitudes for IP and RIP would be measurement-dependent and lost if the test subject changed position. This was evident from the data used in this work.

These results show that IP and RIP can track respiratory volume trends without calibration. RIP is more accurate than IP but requires extra sensors whereas IP can be measured simultaneously with ECG using the same electrodes. Furthermore, the developed SQI method improved correlation between the reference

and IP measurement. The relative volume information is lost with posture change, but new volume tracking could be started based on other sensors detection of the event. However, to confirm the conclusion, the methods should be tested in real hospital environment with longer measurements.

Bibliography

[1] L. A. Lynn and J. P. Curry. "Patterns of unexpected in-hospital deaths: a root cause analysis". In: *Patient Safety in Surgery* 5.3 (2011).

[2] M. Ramsay. "Monitoring Respiratory Rate". In: *Monitoring Technologies in Acute Care Environments: A Comprehensive Guide to Patient Monitoring Technology*. Ed. by M. J. Ehrenfeld and M. Cannesson. New York, NY: Springer New York, 2014, pp. 207–216.

[3] M. A. Cretikos et al. "Respiratory rate: the neglected vital sign". In: *Medical Journal of Australia* 188.11 (2008), p. 657.

[4] K. Holley et al. "Monitoring minute ventilation versus respiratory rate to measure the adequacy of ventilation in patients undergoing upper endoscopic procedures". In: *Journal of Clinical Monitoring and Computing* 30.1 (2016), pp. 33–39.

[5] E. S. Fu et al. "Supplemental oxygen impairs detection of hypoventilation by pulse oximetry". In: *Chest Journal* 126.5 (2004), pp. 1552–1558.

[6] V.-P. Seppä. "Development and Clinical Application of Impedance Pneumography". In: *Tampereen teknillinen yliopisto. Julkaisu – Tampere University of Technology. Publication; 1253* (2014).

[7] C. Voscopoulos et al. "Evaluation of a novel noninvasive respiration monitor providing continuous measurement of minute ventilation in ambulatory subjects in a variety of clinical scenarios". In: *Anesthesia & Analgesia* 117.1 (2013), pp. 91–100.

[8] G. J. Tortora and B. H. Derrickson. *Principles of Anatomy and Physiology*. John Wiley & Sons, 2008.

[9] LadyofHats. *Respiratory system complete en.svg*. Dec. 13, 2007. `https://commons.wikimedia.org/wiki/File:Respiratory_system_complete_en.svg` (accessed Oct. 7, 2016).

[10] D. D. Sin et al. "Risk factors for central and obstructive sleep apnea in 450 men and women with congestive heart failure". In: *American Journal of Respiratory and Critical Care Medicine* 160.4 (1999), pp. 1101–1106.

[11] S. A. Chung, H. Yuan, and F. Chung. "A systemic review of obstructive sleep apnea and its implications for anesthesiologists". In: *Anesthesia & Analgesia* 107.5 (2008), pp. 1543–1563.

[12] S. A. Kofoed and J. A. Orr. *Differential pressure sensor for respiratory monitoring*. US Patent 5,379,650. Jan. 1995.

[13] A. Brahme. *Comprehensive Biomedical Physics*. Newnes, 2014.

[14] A. K. Gupta. "Respiration rate measurement based on impedance pneumography". In: *Texas Instruments application report SBAA181* (2011).

[15] V.-P. Seppä et al. "Novel electrode configuration for highly linear impedance pneumography". In: *Biomedizinische Technik/Biomedical Engineering* 58.1 (2013), pp. 35–38.

[16] M. Młyńczak et al. "Verification of the respiratory parameters derived from impedance pneumography during normal and deep breathing in three body postures". In: *6th European Conference of the International Federation for Medical and Biological Engineering*. Springer. 2015, pp. 881–884.

[17] A. Grenvik et al. "Impedance pneumography : Comparison between chest impedance changes and respiratory volumes in 11 healthy volunteers". In: *Chest* 62.4 (1972), pp. 439–443.

[18] W. Kubicek, E. Kinnen, and A. Edin. "Calibration of an impedance pneumograph". In: *Journal of Applied Physiology* 19.3 (1964), pp. 557–560.

[19] D. Hess. *Respiratory Care: Principles and Practice*. Jones & Bartlett Learning, 2011.

[20] J. Malmivuo and R. Plonsey. *Bioelectromagnetism: principles and applications of bioelectric and biomagnetic fields*. Oxford University Press, USA, 1995.

[21] Z. Zhang et al. "Development of a respiratory inductive plethysmography module supporting multiple sensors for wearable systems". In: *Sensors* 12.10 (2012), pp. 13167–13184.

[22] P. Zimmerman et al. "Postural Changes in Rib Cage and Abdominal Volume-Motion Coefficients and Their Effect on the Calibration of a Respiratory Inductance Plethysmograph 1–3". In: *American Review of Respiratory Disease* 127.2 (1983), pp. 209–214.

[23] P. Várady, S. Bongár, and Z. Benyó. "Detection of airway obstructions and sleep apnea by analyzing the phase relation of respiration movement signals". In: *IEEE Transactions on Instrumentation and Measurement* 52.1 (2003), pp. 2–6.

[24] B. A. Staats et al. “Chest Wall Motion in Sleep Apnea 1, 2”. In: *American Review of Respiratory Disease* 130.1 (1984), pp. 59–63.

[25] J. Hammer, C. Newth, and T. Deakers. “Validation of the phase angle technique as an objective measure of upper airway obstruction”. In: *Pediatric Pulmonology* 19.3 (1995), pp. 167–173.

[26] R. B. Berry. *Fundamentals of Sleep Medicine*. Elsevier Health Sciences, 2011.

[27] R. T. Brouillette et al. “Comparison of respiratory inductive plethysmography and thoracic impedance for apnea monitoring”. In: *The Journal of Pediatrics* 111.3 (1987), pp. 377–383.

[28] F. Q. AL-Khalidi et al. “Respiration rate monitoring methods: a review”. In: *Pediatric Pulmonology* 46.6 (2011), pp. 523–529.

[29] R. G. Soto et al. “Capnography accurately detects apnea during monitored anesthesia care”. In: *Anesthesia & Analgesia* 99.2 (2004), pp. 379–382.

[30] J. A. Hirsch and B. Bishop. “Respiratory sinus arrhythmia in humans: how breathing pattern modulates heart rate”. In: *American Journal of Physiology-Heart and Circulatory Physiology* 241.4 (1981), H620–H629.

[31] L. M. Nilsson. “Respiration signals from photoplethysmography”. In: *Anesthesia & Analgesia* 117.4 (2013), pp. 859–865.

[32] G. B. Moody et al. “Derivation of respiratory signals from multi-lead ECGs”. In: *Computers in Cardiology* 12.1985 (1985), pp. 113–116.

[33] M. Uenoyama et al. “Non-contact respiratory monitoring system using a ceiling-attached microwave antenna”. In: *Medical and Biological Engineering and Computing* 44.9 (2006), pp. 835–840.

[34] J. Xia and R. A. Siochi. “A real-time respiratory motion monitoring system using KINECT: proof of concept”. In: *Medical Physics* 39.5 (2012), pp. 2682–2685.

[35] A. Okss, A. Katasevs, and J. Litvak. “Knitted Resistive Fabric: Properties and Applications”. In: *Rigas Tehniskas Universitates Zinatniskie Raksti* 9 (2014), pp. 28–33.